Heliyon 10 (2024) e26846

Contents lists available at ScienceDirect

Heliyon

journal homepage: www.cell.com/heliyon

Research article

Feasibility study for test rig assessments of fish passage conditions in a Kaplan turbine

Pedro Romero-Gomez [a,*], Aljon Salalila [b], Z. Daniel Deng [b,c], Rudolf Peyreder [a]

[a] Research and Development, Andritz HYDRO GmbH, Linz, Austria
[b] Pacific Northwest National Laboratory, Richland, WA, USA
[c] Department of Mechanical Engineering, Virginia Tech, Blacksburg, VA, 24061, USA

ARTICLE INFO

Keywords:
Kaplan turbine
Test rig
Sensor fish
Fish passage

ABSTRACT

The assessment of fish passage conditions in hydroelectric turbines consists of identifying and quantifying physical magnitudes leading to increased risks of injury of fish passing through turbines in operation. Such assessments are usually carried out either with the use of computer-based methods during design or with field testing of live fish and sensors passing through prototypes. A method in between consists of test rig experimentation, which is critical for testing fish-focused design concepts and offers the opportunity for implementing the most effective design measures for improved fish survivability. However, fish-related assessments in test rigs are not sufficiently documented for industrial applications. This work presents the main findings of an experimental campaign to quantify fish-related hydraulic magnitudes in a physical model of a Kaplan turbine in a commercial test rig. Two operating conditions were tested by releasing miniaturized autonomous sensor devices (termed Sensor Fish Mini) at the turbine intake flow, passing them through the runner in motion and recovering them at the draft tube exit. During passage, time series of acceleration, absolute pressure and rotational velocity were recorded. The recordings were then interpreted to determine the magnitude and likely location of hydraulic stressors hazardous to fish. The statistical tests on the reported measurements indicated that low pressure, collisions on the runner and rotations in the draft tube were not different between the two tested operating points. On the other hand, pressure drop and collision rates on the distributor differed considerably as a function of net head. The outcomes of this investigation showed that test rig evaluations of fish-related properties with Sensor Fish Mini can contribute to an evidence-based development of turbine geometries designed for providing safer passage conditions. Future work will investigate the scaling of test rig measurements to hydraulically equivalent magnitudes in the prototype and their biological consequences.

1. Introduction

1.1. Background

The preservation of aquatic biodiversity has been identified as one of the highest priorities to make hydroelectric production environmentally sustainable while meeting power demands [21]. A mechanistic understanding of the ecological impacts caused by the

* Corresponding author.
E-mail address: pedro.romero-gomez@andritz.com (P. Romero-Gomez).

https://doi.org/10.1016/j.heliyon.2024.e26846
Received 28 November 2023; Received in revised form 2 February 2024; Accepted 20 February 2024
Available online 2 March 2024

construction and operation of hydropower plants (HPP) is essential to increase sustainability and public acceptance of hydropower [9]. To implement effective strategies that minimize adverse effects of HPPs to fish and other forms of aquatic life in rivers, hydropower stakeholders rely primarily on environmental assessments of fish population and fish survival estimates in affected water bodies. Regarding turbine passage, for instance, mortality rates of fish passing turbines have been measured onsite with live fish deployed through operating turbines, and were estimated to be 8.7% ± 1.1% (SE, N = 138) and 28.5% ± 1.6% (SE, N = 276) in Kaplan and Francis units, based on experiments with thirteen and twenty taxa, respectively [25]. A consensus has been reached that the current status of turbine technology can be considerably improved to minimize mortality rates via enhanced design and strategic operations [30]. The correlation between design/operations and the likelihood of fish survival is mostly dictated by the magnitude of key hydraulic conditions that have been identified as the leading cause of mortal injury [7,11]. A protocol was developed to identify and characterize injury types and health status of fish that were passed through prototype turbines, which accounted for spine damages, amputations, hemorrhages, emboli, scale loss, vitality, among other criteria that were visible in the examination of 5349 individuals of 36 hatchery-reared and wild fish species [22]. Linking the mechanical/hydraulic stress to a specific injury via X-rays constituted another significant advancement in our understanding of the role that turbine hydraulic conditions play in passage survival [23]. For instance, swim bladder rupture is linked to rapid pressure changes whereas fractures are linked to blade strike. It has been suggested that strategic turbine design concepts can steer key turbine hydraulic magnitudes to achieve significant improvements in fish passage conditions. Quantifications of hydraulic stressors are usually conducted either with computer-based assessments in the design phase or with field testing of prototypes with Sensor Fish. We formulated the hypothesis that experimentation in test rigs, via deployments of sensors through a physical model of the interrogated turbine, can bridge the computer- and field-based methods. To test our hypothesis, we proposed herein an experimental workflow to sample passage conditions and discussed the outcomes from a measurement campaign.

A body of literature has identified hydraulic stressors that increase risks of mortal injury for fish passing turbines in operation. A comprehensive review [7] pointed the significant role of mechanical strike, pressure, cavitation and shear flows as sources of mortal injury in various species. Fundamental concepts were proposed [6] to explore the possibility to minimize injuries on fish through enhanced geometric designs, to emphasize the need for quantification of specific injury mechanisms, and to relate fish survival and operational efficiency. Mature hydro projects where turbines were developed for enhanced fish passage were summarized and discussed for their effectiveness, and were the basis to refine turbine designs in subsequent rehabilitation projects with stricter environmental goals [12]. On the side of biological investigations, the contribution of [25] summarized studies for quantifying direct fish passage survival, which consist of passing samples of live fish through turbines, a technique that has been already implemented for decades. Important in the latter meta-study was the solid reference it provided about the mean survival rates for typical target species in Francis-, Kaplan- and crossflow-type machines. The work of [5] put emphasis on barotrauma-related injuries resulting from the rapid pressure changes through turbines and provided a research pathway for adaptive management based on ecology, behavioral, onsite, laboratory and modelling studies. A common element from the cited studies is the idea that quantitative assessments of fish survival begin with an accurate evaluation of hydraulic conditions through turbines. A growing body of literature has produced evidence that field testing of fish-related hydraulic stressors with autonomous sensors (Sensor Fish) can characterize turbine design and operations from a biological standpoint [3,17–20]. In the facilities of turbine manufacturers and research institutions worldwide, test rig experimentation is extensively conducted to examine flow phenomena for fulfilling hydraulic performance guarantees. This feasibility study demonstrated that current hydraulic investigations in commercial and research test rigs can be conveniently adapted for concurrent evaluations of fish-related hydraulic metrics.

1.2. Motivation for fish passage experiments in test rigs: the turbine design process

We describe herein the prominent role that test rig experimentation plays in turbine design and why it offers an opportunity for enhancing fish passage. At the outset of any design project, turbine engineers use reference turbine geometries and component configurations to conduct a so-called hydraulic layout, that is, to define a design candidate that has the potential to fulfill hydraulic guarantees. Next, a phase called hydraulic development thoroughly examines flow phenomena by means of computational fluid dynamics techniques. The use of these simulated flow conditions for fish passage assessments was an important development that offered the possibility for turbine industry to contribute to the field of turbine passage. Initially formulated by Ref. [31], the conceptual framework for simulation-based fish passage assessments led to the development of a model-based biological performance assessment (BioPA) toolset for comparative studies of survival of fish passing turbine flows [26]. In this desktop-based method, velocity, turbulence and pressure fields from flow simulations served as information basis that feeds into biological response models. Following this paradigm, flow simulations were used to investigate the hydraulic parameters affecting fish survival through a vortex power plant equipped with a Francis-type turbine [24], whereas another work [15] represented fish trajectories with streamlines generated on simulated flow conditions to investigate the influence of shear, collision and barotrauma on the survival of European eels (*Anguilla anguilla*). Computer-based techniques provide a solid ground for early estimates during the design process, a phase where substantial geometric changes can be made for increasing fish passage survivability.

After flow simulations are conducted in turbine design, the next step consists of validating flow phenomena via hydraulic test rig experimentations in physical (scaled) models of the candidate designs. The long-standing practice of testing hydroelectric turbines gave rise to well-established protocols and standards with which most commercial turbine developers comply (e.g. IEC- 60193 [14]). Test rig experiments are conducted to demonstrate that efficiencies are guaranteed, that performance is optimal, and that operations avoid the appearance of undesirable phenomena such as cavitation and pressure pulsations which could compromise mechanical integrity. Regarding fish passage evaluations, comparative studies in a test rig could facilitate an evidence-based, data-driven

assessment of passage conditions. However, test rig-based studies observing fish-related hydraulics are scant and not fully accessible in the technical literature. Filling this knowledge gap is the main goal of the present work. We achieved the main goal by (i) proposing a test rig method based on recordings with Sensor Fish Mini and, (ii) implementing the proposed method in the comparative analysis of two operating points with distinct flow passage conditions. The structure of this article therefore consists of a summary of the investigated hydraulic stressors, the description of the test rig and the interrogated physical model, a thorough outline of the deployment procedure as well as the tested operating points, and the presentation of results and analyses of collected data.

2. Material and method

2.1. Investigated fish-related hydraulic stressors of turbines

The experimental campaign measured the following hydraulic stressors in conformity with general practices for deployments of standard sensor fish in prototypes of large turbines as well as in low-head turbines [3,17–20]. The list of collected key hydraulic measurements, as well as arguments as to why they were selected, is as follows.

- Nadir pressure (P_{nadir}) and pressure change (ΔP): Fish can adapt to changes in pressure in their surrounding environment, but tolerable changes must take place at a much slower rate than the sudden pressure drops observed during turbine passage. In biological studies, the lowest pressure recorded during turbine passage (nadir) and the pressure at which fish were acclimated right before passage (acclimation depth or pressure [16]) were driving factors for the extent of mortality. It has been observed that mortality increases with greater differences between acclimation and the lowest pressures experienced by tested fish samples [4]. Therefore, the present campaign measured the minimum absolute pressure (nadir) as well as the magnitude of the pressure change (ΔP) of each sensor passage through the turbine.
- Maximum acceleration events (a_{mag}): acceleration/deceleration events of passing sensors signal (i) rapid changes in flow conditions and (ii) significant blade strikes. The measurement campaign reported herein focused on acceleration events of the second type since they are known to be of biological significance. Laboratory data were generated [1] to quantify survival rates to blade strike of rainbow trout (*Oncorhynchus mykiss*) as a function of the fish length, the thickness ratio and the impact velocity, while the contribution of [29] expanded the analysis to account for the influence of the strike angle and location on the fish body. Both sensors and live fish were subjected to the same impact condition [2], which allowed for the development of a correlation between the impact velocity and the acceleration data collected by sensors.
- Integral of rotational velocity (Ω): this metric is influenced by the presence of high levels of turbulence. Laboratory experiments were conducted with live spring Chinook salmon (*Oncorhynchus tshawytscha*) subjected to two conditions of high turbulence generated with jet arrays [10]. The test condition was the exposure time and the experimental outcomes indicated a tendency for fish to take longer time to reorient themselves with longer exposure periods. This increased disorientation of passing fish has been qualitatively associated with increased likelihood of predation after passage (also called indirect mortality [7]). Therefore, the

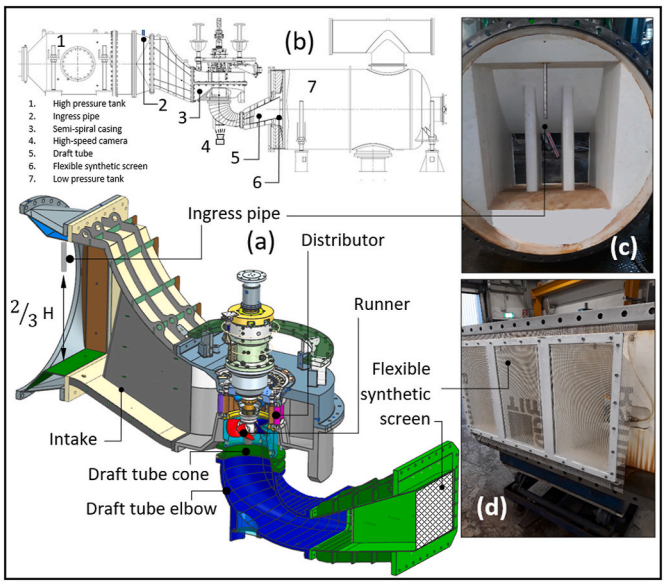

Fig. 1. The physical model of the Kaplan turbine (a) was hydraulically investigated in a close-loop test rig (b). The installation of the ingress pipe at the intake (c) and the stoppage screen at the draft tube outlet (d) were the main modifications to accommodate the testing with SF Mini. The ingress pipe exit was located at an elevation equal to two-thirds of the cross-section height (H).

notion has emerged that the levels of turbulence (or of its surrogate metric recorded herein, namely the rotational velocity) should be preferably reduced to minimize risks of indirect mortality.

2.2. The test rig

Experiments were conducted in a test rig facility of Andritz HYDRO GmbH located in Linz (Austria) (Fig. 1). It is aclosed-loop hydraulic system for commercial projects in which the pressure differential through the interrogated turbine can be highly controlled to match a hydraulically equivalent head in the field (Fig. 1b). A variable-speed pump supplies water through the turbine at a scaled flow rate that was hydraulically equivalent to the discharge in the prototype. The equivalence of both the hydraulic head and discharge was established through hydraulic similarity. The model was homologous to the prototype and featured a full-spiral type intake, a distributor with stay vanes and 24 guide vanes, a Kaplan runner with five blades and an elbow-type draft tube of varying cross-section with two piers (Fig. 1a). The interrogated model of the Kaplan runner (diameter of 34 cm) was a candidate design for a commercial project and was thoroughly tested in compliance with calibration and measuring protocols of the IEC- 60193 standards for model acceptance of hydraulic turbines and pump-turbines [14]. Given the nature of the usual hydraulic testing conducted in this test rig (protocol-based, standardized, certified according to ISO standards), we can state that the experimental apparatus is a standard facility available to major turbine manufacturers supplying electromechanical equipment to hydropower plants, and to various laboratories for hydraulic machinery research. This, in turn, ensures the repeatability of the proposed approach.

Two main adaptations were made to conduct the experiments. The first modification consisted of a rigid stainless-steel pipe of 27-mm diameter installed immediately before the intake section of the physical model (see Fig. 1c). Two plug valves allowed the introduction of the SF Mini into the upper portion of the ingress pipe. A regulated water jet from a booster pump pushed the sensors downwards. The elevation of the bottom pipe end defined the location where sensors entered the intake flow and corresponded to two-thirds of the height (H) of the local cross section. The second modification consisted of a flexible synthetic screen that was attached to the end of the draft tube piers to prevent the sensors from traveling further into the closed loop (Fig. 1d). These were the only modifications to the physical model that departed from a conventional testing for hydraulic performance.

2.3. The Sensor Fish Mini and surrogate spheres

The Sensor Fish Mini (SF Mini) is an autonomous device designed at the Pacific Northwest National Laboratory (PNNL, Richland, WA. U.S.A) to record hydraulic conditions during passage through flows influenced by hydraulic infrastructure [8]. The SF technology was developed to conduct in-situ measurements of hazardous flow conditions that migratory fish often encounter during passage of a hydropower plant. The "SF Mini" is a further development of the SF that features a considerably smaller size (nearly spherical with diameter of 23 mm, 6.4 g) than the standard SF (nearly cylindrical with diameter of 25 mm and height of 90 mm, weight of 42 g). This allows deployments in small infrastructures [28]. The SF Mini can collect 2.5 min of the following measurements at a sampling rate of 2048 Hz.

- Linear acceleration (3 components): analog accelerometer with ±200 g range (g is earth's gravity)
- Pressure: board mount unit, maximum value of 1200 kPa
- Rotational rate of change (three components): magnetometer ($\pm 2000^{\circ}\ s^{-1}$)

The SF Mini is nearly neutrally buoyant in water, has a flash memory of 64 Mbit and a Lithium battery of 50 mA h, operating with a voltage of 2.7–3.6 V.

Prior to the deployment of the measuring units, we released hollow spheres of 23-mm diameter specially fabricated for this study out of Aluminum AlSi10Mg with a shell thickness that made the spheres neutrally buoyant. The hollow spheres were released before the SF Mini to ensure that the physical model of the turbine, the test rig instrumentation and the SF Mini do not suffer any major damage. In addition, these preliminary releases allowed us to test the ability to record the passage of an object through the runner region with a camera system (see item 4 in Fig. 1b, below the draft tube elbow).

2.4. The deployment procedure and operating points

Five SF Mini and twelve surrogate spheres were available for the experimentation and a release/retrieval strategy was implemented as follows. Each SF Mini was introduced individually into the upper portion of the ingress pipe between the two plug valves in closed modus. A hose connected to a booster pump was fastened, the booster pump was switched on and the upstream plug valve was opened. The downstream plug valve was slightly open to let residual air flow through the unit. After the recording delay time (T_d) elapsed, the downstream plug valve was fully open to push the sensor downwards. Sensor recordings showed that the ingress process took approximately 30 s to the pipe exit. Booster pump flow rates contributed minimally to the flow rate through the unit. Runner passage was recorded with a high-speed camera (Mikrotron EoSens Cube7 from Mikrotron GmbH, Unterschleissheim, Germany) installed at the lowest point of the draft tube (below the elbow) and looking up towards to the runner. The camera used a lens (Pentax F1.0-22, f = 8–48 mm, C-Mount) and required special lighting with four light fixtures (ST-MHK-HiB) and one control unit (ST-MH-N2). One video recording of a sensor passage is available in the supplementary material of the present article. After all intended units (sensor or spheres) passed, the physical model was dewatered, the draft tube end was disassembled from the lower tank, both sensors and hollow spheres were collected, the draft tube was assembled again, and the unit was pressurized and made ready for the next set of

deployments.

The operating conditions tested in the experiments corresponded to two ONCAM points of machine operation at the low (OP1) and rated (OP2) heads (indicated in Fig. 2). Fig. 2 is an analogous schematic of the actual hill chart and shows that OP1 and OP2 lie near the operational limit at high discharge. In the hydraulic performance of a physical model, operating points are defined in terms of the speed (n_{ED}) and discharge (Q_{ED}) factors, where Q is the discharge (m^3/s), H is net head (m), D is the nominal runner diameter (m), g is gravity acceleration (m/s^2), and n is the rotational speed of the runner (revolutions per second):

$$Q_{ED} = \frac{Q}{D^2\sqrt{gH}}$$

$$n_{ED} = \frac{nD}{\sqrt{gH}}$$

Under hydraulic similarity, two geometrically identical machines of different scale (e.g., a small physical model in a test rig and the homologous prototype in the power plant) produce nearly equivalent hydraulic phenomena if operated at the same Q_{ED} and n_{ED} [14]. In this work, the horizonal and vertical axes of the hill chart in Fig. 2 present the values of n_{ED} and Q_{ED} over the entire operating range in a normalized manner (n_{ED}* and Q_{ED}*) with respect to the corresponding values at the best operating point (BEP). The tested operating points (OP1 and OP2) were defined near the cavitating region at high discharge because various studies have indicated that high discharges tend to give rise to hazardous pressures [27]. Furthermore, high discharges allowed for greater guide vane openings which minimized the likelihood that the SF Mini, which are relatively big for the guide vane passage gaps, were retained during distributor passage. From the sixty-five releases (thirty-seven releases of SF Mini and twenty-eight releases of surrogate spheres), only one instance did not pass through the distributor and had to be recovered in the casing. The sample size (number of passage events per operating point) collected with the SF Mini were twenty-two and fifteen for OP1 and OP2, correspondingly.

2.5. Data post-processing and statistical tests

The sensor data post-processing was carried out using functionalities of the Hydropower Biological Evaluation Toolset (HBET) [13]. HBET was developed to assist in designing field and laboratory tests with SF and to facilitate data analyses of SF recordings. HBET converts raw SF data into standard formatting (csv files), which allowed us to conduct complementary implementations of algorithms with other programming languages (MATLAB®) to identify physical locations (region) where magnitudes of interest take place. From the investigated hydraulic stressors described in section 1.3, statistics for nadir pressure and significant acceleration events per region were post-processed with HBET, whereas the integral of rotational velocity magnitude was calculated with MATLAB. Pressures (P*), pressure drops (ΔP*), rotational velocities (ω^*_{mag}), and integrals of rotational velocity (Ω*) are defined by equations (1)–(4), normalized by references values (P_{max}, P_{min}, ΔP_{max}, $\omega_{mag,ref}$ and Ω_{ref}) that were valid for all results presented in this study. SF already provide acceleration magnitudes normalized with respect to Earth's gravity.

$$P^* = \frac{P - P_{min}}{P_{max} - P_{min}} \tag{1}$$

$$\Delta P^* = \frac{\Delta P}{\Delta P_{max}} \tag{2}$$

$$\omega^*_{mag} = \frac{\omega_{mag}}{\omega_{mag,ref}} \tag{3}$$

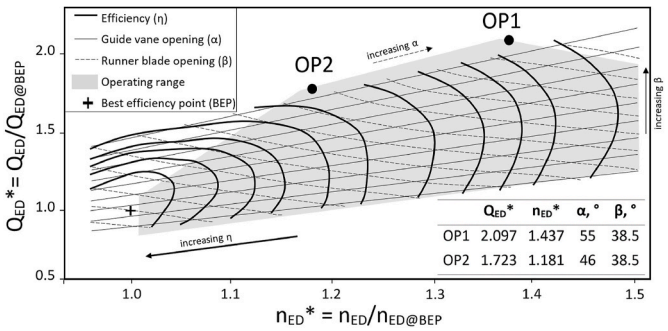

Fig. 2. Schematic of the hill chart of the interrogated Kaplan turbine and components. The inset table shows details about the interrogated operating points. The efficiency (η) of the turbine is presented with respect to dimensionless values of the discharge factor (Q_{ED}) and the speed factor (n_{ED}).

$$\Omega^* = \frac{\Omega}{\Omega_{ref}} \tag{4}$$

The integral of rotational velocity (Ω) in eq. (4) was calculated per passage region (guide vane, runner and draft tube) using the trapezoidal rule (eq. (5)). Passage periods were bounded by time markings (T_i, see section 3.1) visually selected via HBET. The integral Ω over a passage period contained *n* recordings at equal time intervals ($\Delta t = (T_{i+1} - T_i)/n$) and was defined as:

$$\int_{T_i}^{T_{i+1}} \omega_{mag}(t)\, dt \approx \Omega = \frac{\Delta t}{2}\left[\omega_{mag}(t_0) + 2\omega_{mag}(t_1) + 2\omega_{mag}(t_2) + \ldots + 2\omega_{mag}(t_{n-1}) + \omega_{mag}(t_n)\right]. \tag{5}$$

The reported pressure values (P* and ΔP*) as well as the rotation integral per passage region (Ω) are presented as cumulative distributions from all sampled values for each operating point.

Statistical tests were run on the experimental outcomes to either accept or reject the null hypothesis (H_0) that passage conditions were the same in both operating conditions.

- To test the distributions of nadir pressures and values of integral Ω, a two-sample Kolmogorov-Smirnov (K–S) statistical test was run under a significance level (α) equal to 5% (0.05) and the test also provided the asymptotic confidence value (p-value).
- To test the collision rates, a "two proportions" statistical test was run under a significance level (α) equal to 5% (0.05)

3. Results and discussion

3.1. Example of turbine passage events based on collected SF mini data

One example of the collected datasets is presented in Fig. 3 as time series of normalized pressure (P*), the magnitude of linear acceleration (a_{mag}) and the magnitude of angular rate of change (ω^*_{mag}). The features and trends of the magnitudes presented in Fig. 3 were very consistent across all datasets. The SF Mini does not record its spatial position, which means that location must be inferred based on identifiable features of the time series. A reference for such features was known from empirical observations in previous analyses of SF data as well as from equivalent time series from streamlines on computer-simulated flow fields. For the simulation-based method, the geometric model of the turbine was digitized and used to calculate the three-dimensional distributions of velocity, pressure and turbulent parameters. The simulations of the two operating points were based on computational fluid dynamics, a technique that is routinely implemented for the development of new turbine geometries in industry settings. The use of CFD

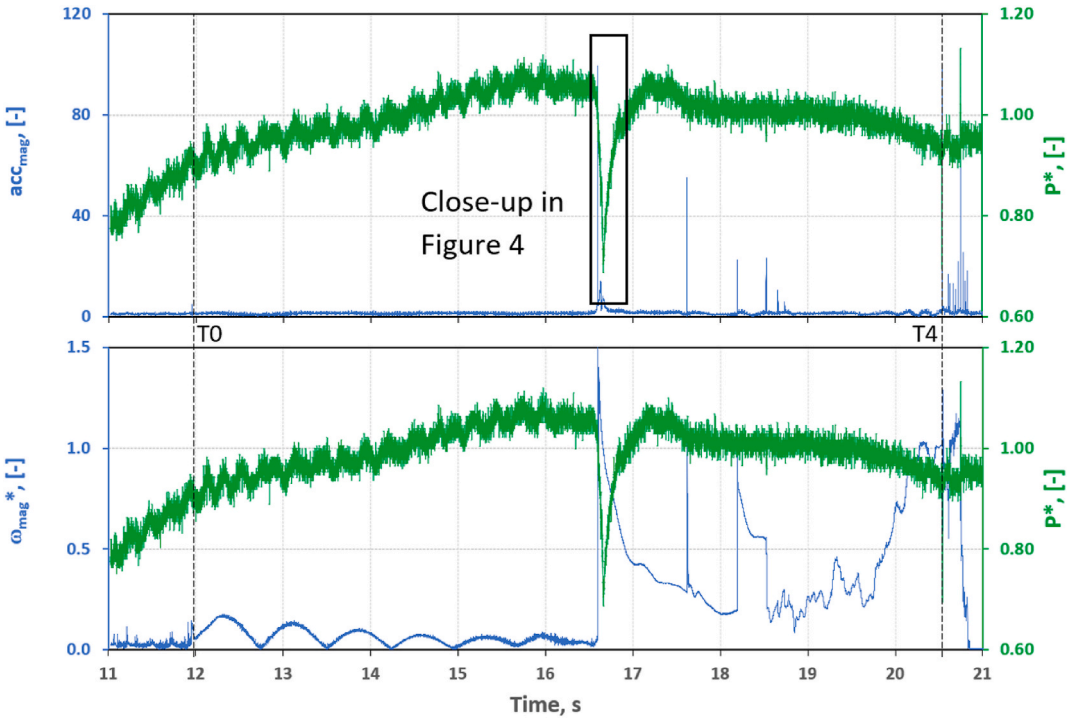

Fig. 3. Time series of absolute pressure (P*), the magnitude of linear acceleration (acc_{mag}) and the magnitude of angular rate of change (ω^*_{mag}) collected from one SF Mini passage through the interrogated Kaplan turbine at OP1. These time series show the time markings for the instant of ingress into the intake flow (T0) and the end of draft tube (T4).

simulations for evaluating fish passage conditions have recently found favor also with researchers and operators [15],[23],[26]. With the simulated flow fields for OP1 and OP2, streamlines were generated to represent trajectories of moving SF Mini. Along the trajectories, absolute pressure values can be extracted to produce time series analogous to the experimental time series. One example of the CFD-based pressure data is shown in the inset of Fig. 4. Unlike SF Mini data, CFD-generated trajectories yielded the spatial locations of hydraulic stressors. In a conventional design project, CFD techniques are intensively deployed in the initial phase and, therefore, can assist in fulfilling fish-related specifications or guarantees in case these were contractually stipulated. Additionally, SF Mini data may serve as a baseline to evaluate the accuracy of CFD-generated hydraulic stressor magnitudes. Time markings (T0, T1, T2, T3 and T4 in Figs. 3 and 4) on SF-measured time series defined spatial regions as follows.

- The instant of ingress (T0) was identified at the onset of an oscillatory mode of ω^*_{mag}, which derived from the influence of the wake flow on the drag torque. Drag torque arose from the differential velocity between the spinning sphere surface and the surrounding fluid. The periodicity of the vortex shedding arising from the pipe end made ω^*_{mag} fluctuate regularly in the transect between the ingress and the entry to the distributor. The oscillation amplitude had its greatest value as SF Mini exited the ingress pipe and decreased gradually after ingress. Acceleration recordings indicated that contact events of any kind (mild or severe) were absent at the intake and that oscillations in acceleration magnitude were always mild (below 5 g). Absolute pressure recordings increased continuously until a maximum value was reached (P_{max}*).
- The entrance to the distributor (T1) was characterized by P_{max}* and, more precisely, by a mild pressure drop, which was also appreciable in the CFD-based time series of pressure shown in the inset of Fig. 4. Both streamlines and sensor data indicated that at the entry to the distributor, fluid accelerations resulted in an increment of kinetic energy and, consequently, in a slight drop in pressure. This pattern was attested in nearly all sensors and streamlines. P* decreased further during the short passage time through the guide vanes, with greater rates of pressure change observed towards the runner region.
- The entry to the runner (T2) was inferred based on the CFD-based outcome that minimum P* values (the nadir pressure for each passage) correlated well with a position below the runner blades [27]. Therefore, T2 was calculated as the time where nadir pressure occurred (from the sensor signal) minus the average residence time (from CFD-based streamlines) elapsed between the entrance to the runner region and the occurrence of the minimum (nadir) pressure.
- The entry to the draft tube (T3) can be inferred in a similar manner as T2, i.e., T3 was calculated as the time where nadir pressure occurred (from the sensor signal) plus the average residence time (from CFD-based streamlines) elapsed between the occurrence of the minimum (nadir) pressure and the entrance to the draft tube. After T3, most SF data series feature a pressure recovery process until a local maximum value was reached at the draft tube elbow. In addition, turbulent conditions in the draft tube passage triggered high values of rotational speed (ω^*_{mag}).
- The end of passage (T4) was selected when a sudden drop in ω^*_{mag} was observed in SF data, concurrent with spikes of the magnitude of linear acceleration (a_{mag}). This combination of events indicated the occurrence of sensor collisions with full force on the stopping net installed at the draft tube exit (Fig. 1d)

Most sensors yielded time series that showed the abovementioned features, with only a few exhibiting minor deviations. For instance, some SF did not record a very strong, regular fluctuating angular velocity at the instant of ingress, but T0 was determined as the instant when acceleration spikes caused by collisions inside the ingress pipe disappear. Other SF recorded a relatively flat time

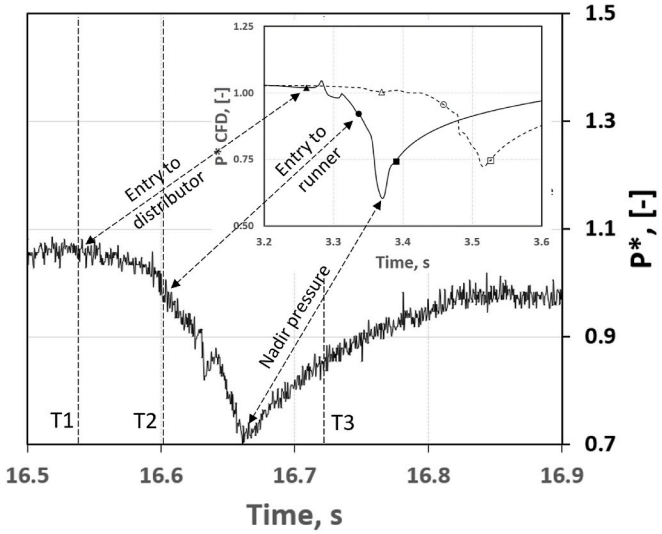

Fig. 4. Close-up of Fig. 3 near the nadir pressure to indicate the time markings for the entry to distributor (T1), the entry to runner (T2) and entry to draft tube (T3). The inset shows equivalent time series of dimensionless absolute pressure (P*) generated with streamlines in flow simulations of the operating points investigated in the test rig. Only results from two streamlines are shown in the inset.

series of absolute pressure from ingress to the distributor. This, however, did not preclude the selection of the time markings that were necessary for data analyses.

3.2. Radial and tangential location of runner passage

The video recordings with the high-speed camera were post-processed to determine spatial distributions of the SF at the instant it crossed the runner, where hazardous collisions may take place. The frames in Fig. 5 corresponded to the instant when sensors and spheres were first observed below the runner and were digitized and the locations normalized with respect to the runner center of rotation and runner diameter. Eight of the frames are shown as examples in Fig. 5a and the collection of passage locations for all is shown in Fig. 5b. The frequency of passage through each quadrant was as follows: high in III, then in I, lower frequency in II and IV. Regarding the radial distribution (Fig. 5c), passages occurred mainly towards the discharge ring. For turbine design teams, the identification of the runner passage location is necessary in the hydraulic development of new runners if fish passage survival must be improved. As summarized by Ref. [12], a notion has emerged that thick leading edges of runner blades together with minimized gaps between runner and discharge ring may reduce the negative effects of fish contacts with runner blades. In design, such modifications are associated with mechanical construction constraints as well as with appearance of undesirable flow phenomena, e.g., cavitation and pressure pulsations. In addition, leading blade edges cannot be made thicker uniformly over the entire radial distance. Due to reasons related to construction, near-hub geometric features offer the greatest opportunity for making blade edges blunter, while radial positions near the discharge ring are more difficult to modify. Therefore, the accurate identification of runner passage allows us to assess the benefits of laborious runner design concepts. This study demonstrated that experimental recordings of passing sensors can be a reliable source of information to carry out the passage location evaluation.

3.3. Nadir pressures and pressure change

To contextualize the trends in nadir pressure measurements, it is essential to recall that a turbine is a mechanical device that extracts work from a system constrained by a hydraulic head. This energy extraction results in an overall pressure drop through the runner. Fig. 6a shows that nadir pressures in both operating points were nearly similar, which was also statistically confirmed by the two-sample modified Kolmogorov-Smirnov test of equal distributions (H_0 was not rejected, p-value = 0.5285). OP1 yielded dimensionless nadir pressure values (minimum–median–maximum of P*) of 0.53–0.68 – 0.74, whereas the equivalent statistical values for the samples collected from OP2 were 0.55–0.65 – 0.77 kPa, respectively. Hydraulically, conditions in OP1 may trigger cavitation with greater likelihood than in OP2. Biologically, cavitation may promote lower nadir pressures, thereby increasing the risks of mortal injury due to barotrauma, an injury mechanism that has been amply documented for migratory fish species [5]. For that reason, turbine engineers should not only observe mean nadir pressure conditions but also thoroughly examine variability that may bring

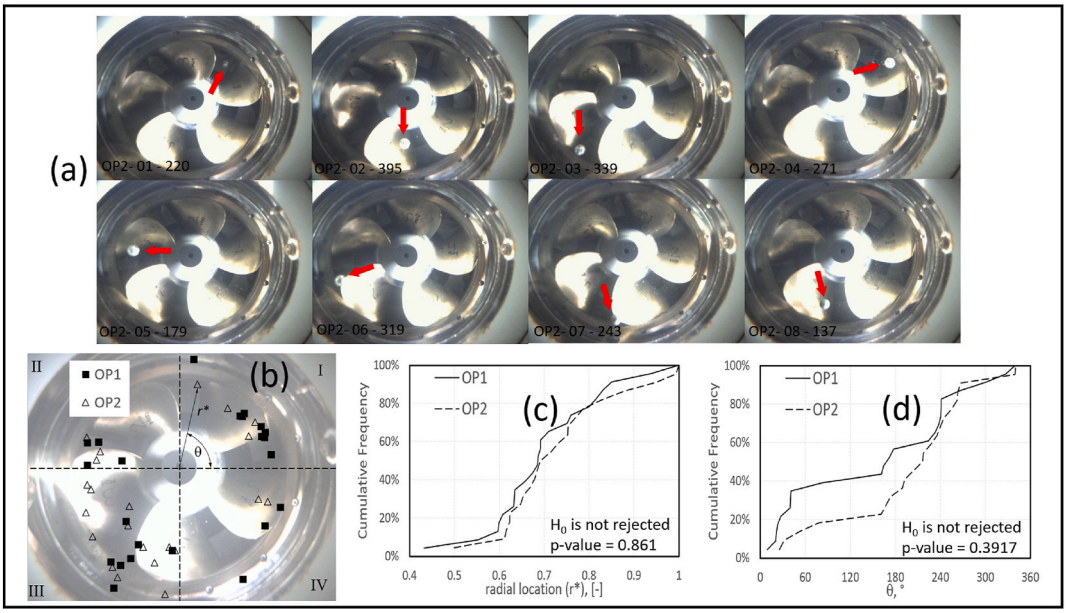

Fig. 5. (a) Examples of the instant when SF Mini passed under the runner blades. (b) Frames were digitized to determine the runner crossing location from all sensors (sphere passage was also included), characterized by the radial (r*) and angular positions (θ). The cumulative frequency distributions of the radial and angular positions are shown in (c) and (d), respectively. Sample sizes were N = 22 and 15 for OP1 and OP2, correspondingly. The outcome of a two-sample Kolmogorov-Smirnov statistical test on both distributions in (c) and (d) is presented, as well as the p-value.

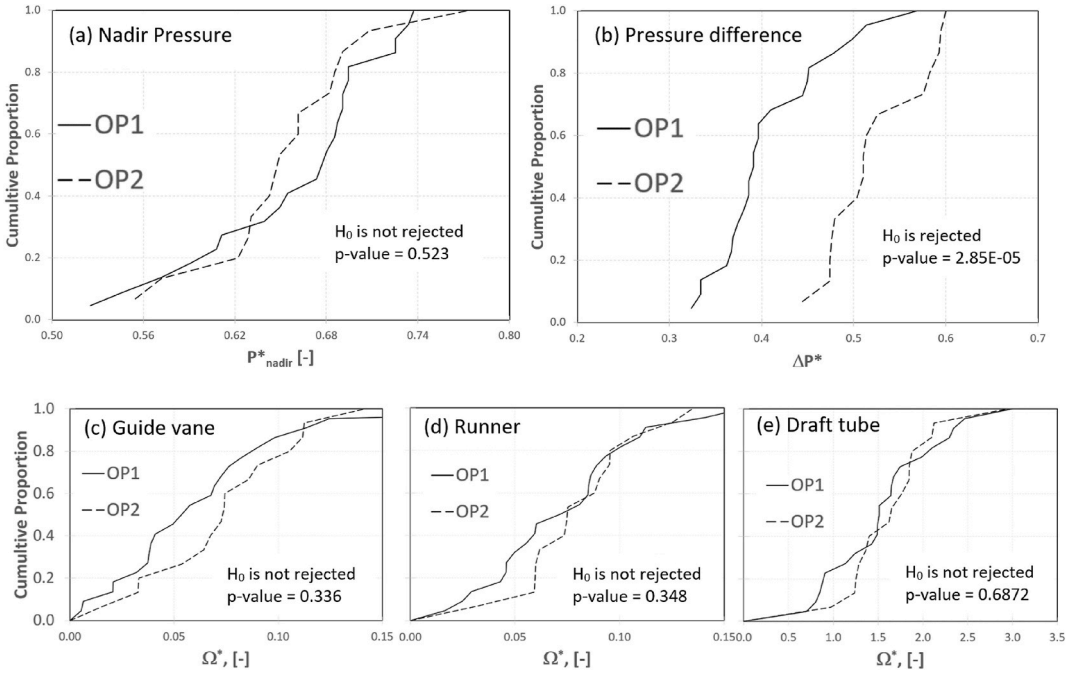

Fig. 6. Cumulative frequency distributions of the (a) nadir pressure (P^*_{nadir}), (b) the pressure differences between pressure at guide vane entry and the nadir pressures (ΔP^*), and (c) the integral of the rotational velocity magnitude (Ω^*) for passage through the guide vane (T1 to T2), (d) through the runner (T2 to T3) and (e) through the draft tube (T3 to T4). Sample sizes were N = 22 and 15 for OP1 and OP2, correspondingly. The outcome of the two-sample Kolmogorov-Smirnov statistical test on both distributions is presented in each plot, as well as the p-value.

nadir pressure values to near cavitating conditions. The cumulative distributions herein are not conclusive as to the prevailing notion that fish passage conditions improve in operating regions towards the best efficiency point (BEP). This premise emerged from the assumption that flow conditions at BEP are hydraulically optimal, which in turn minimizes the risks to fish mortality associated with disrupted flow velocities patterns, high turbulent conditions, and extremely low pressures. Such premise was put to test [27] by estimating collision- and pressure-related risks of mortality at 26 operating points that were nearly uniformly distributed over the operating range of a large Kaplan turbine (runner diameter of 8.5 m, head range of 22 m–35 m, and discharge range of 250–800 m^3/s). In relation to nadir pressure, passage survival of juvenile salmonids was higher in only four of the twenty-six examined operating points than at BEP. However, in relation to collision, passage survival was greater in eighteen out of twenty-six examined OPs than at BEP. This showed that the assumption that BEP is optimal from both a hydraulic and biological standpoint must not be over-generalized. Model- and data-based evaluations of this kind are necessary under a wide range of scenarios (and not only a few reference points) to further provide evidence or disprove commonly accepted notions about passage conditions through turbines.

The magnitude of pressure change (ΔP^*, Fig. 6b) was calculated for each passage event by subtracting the nadir pressure from the recorded pressure at the time of entry to the guide vanes (T1). The ΔP^* reported herein acts as a surrogate of the pressure differential whose magnitude directly influences the risks of mortal injury due to barotrauma for passing fish. The lower the pressure differential is, the higher the likelihood of survival. Fig. 6b indicates that, the higher the hydraulic head was, the higher the ΔP^* tended to be. ΔP^* statistics (minimum – median – maximum) of OP1 were 0.32–0.39 – 0.57, whereas the equivalent metrics for OP2 were 0.44–0.51–0.60, respectively. On the premise that this comparative outcome holds true in an analogous prototype, the passage through the turbine at OP1 can be assumed to be safer than at OP2. The variability of ΔP^* distributions was also greater in OP1 than in OP2.

An important consideration in the analysis of the measured pressures is that the Thoma numbers (σ, cavitation factor) in OP1 and OP2 were higher than the operational plant values. The Thoma number establishes the cavitation condition of the turbine with respect to a critical Thoma number (σ_c) where cavitation appears. Each turbine design has a σ_c value and turbine operations must ensure that $\sigma > \sigma_c$. Because we selected two operating points near the cavitation limit (see Fig. 2), setting σ values to prototype operational values could have induced low pressure values which SF Mini might not have withstood. For that reason, the σ-values in OP1 and OP2 tested in the laboratory were greater than those in the corresponding prototype operations. This does not represent a shortcoming of the experimental method because test rig pressures can always be reconverted to prototype-scaled values based on the premise of hydraulic similarity.

3.4. Acceleration data analysis: collision and contact events

The acceleration recordings signaled rapid changes in the sensor trajectory due to rapidly changing flow conditions and due to collisions/contacts with solid boundaries. While transient flow conditions gave rise to gradually increasing acceleration

measurements, collisions and contacts generated sudden short-term spikes in acceleration recordings. Previous works with standard-size SF units deployed in prototypes have used a criterion of 95 g to classify these spikes as severe contacts [17–20]. Contacts can be classified as either collision and shear events depending on the time span of the acceleration spike. In the present study, all spikes exceeding 95 g turned out to be classified as collisions by HBET. This finding is particular to the present test rig experimentation; in general, SF deployments in prototypes recorded both collision events (spikes with peak durations shorter than 7.5 ms) and shear events (spikes with peak durations longer than 7.5 ms).

The overall percentage of significant events identified by HBET is shown in Table 1. The rates at the intake were distinct between operating conditions and related to sensor interactions with intake/stay vane walls leading towards the distributor. Collisions on the guide vanes were relatively high from both tested OPs due to the narrow passage through the guide vanes (relative to sensor size). The smaller guide vane opening in OP2 ($\alpha = 46°$) yielded greater collision rates than OP1 ($\alpha = 55°$), and this difference was confirmed by the statistical test (H_0 was rejected). Distinct rates were evident at the runner and draft tube, with the OP2 yielding lower values. However, the statistical test was not rejected and collision rates were deemed to be equal, an outcome that was strongly influenced by the relatively small sample size of the present study.

3.5. Integral of rotational velocity magnitude

The rotation integral (Ω, eq. (5)) was determined for each transect of the sensor passage (Fig. 6c, d and 6e for passages through the guide vane, the runner, and the draft tube, respectively). The guide vane passage (T1 to T2, Fig. 6c) shows distribution curves that were different according to the operating condition, with median values of 0.054 and 0.074 for OP1 and OP2, respectively. Two factors influence the rotation integral Ω, namely, the passage time and the rotational velocity. The passage time through the guide vanes (T1 to T2) was essentially the same for both operating points; however, OP2 was set with closer guide vanes ($\alpha = 46°$ for OP2 vs $\alpha = 55°$ for OP1, Fig. 2), which resulted in greater likelihood of collisions. The rotation induced by collisions was short-lived but considerably large. Because guide vane passage time was relatively short (71 ms in both OPs), the recordings captured the influence of the short-term outburst of sensor spinning after collisions took place. This tendency did not propagate to the runner (T2 to T3, Fig. 6d), through which the cumulative distribution curves were essentially the same. As for the draft tube passage, approximately the 75th-percentile of the OP1 events showed lower values than the 75th-percentile of OP2 events. This trend reversed at the 75th-percentile (at $\Omega^* = 1.879$). Notice that Ω^* for the draft tube is one order of magnitude greater than for the guide vane and runner, primarily because of the longer passage time through the runner in comparison to GV and runner passage times, and also due to the much stronger turbulent conditions present in the draft tube.

4. Limitations and contextualization of the present test rig measurements

The present study demonstrated the feasibility of deploying miniaturized sensors in physical models of Kaplan turbines to measure hydraulic conditions that fish may encounter during turbine passage. However, the measurements presented herein represent test rig hydraulic conditions and, therefore, cannot yet be used to evaluate the likelihood of mortal injury due to pressure, collision, and turbulence. A full biological characterization of Kaplan turbines consists of scaling test rig measurements to hydraulically equivalent prototype values and using existing dose-response relationships to estimate survival rates of specific fish species. For the time being, fish passage conditions can be conducted in a comparative manner based on hydraulic stressor magnitudes. The full biological characterization was purposely deferred to future works.

Furthermore, the SF Mini would be considerably large if scaled up to prototype size and this means that outcomes from a SF Mini in the test rig would be equivalent to the stressors experienced by a very large object moving through the prototype. For that reason, further analyses are required to adequately scale up the outcomes from SF Mini units to used them in dose-response relationships for biological characterization of passage.

5. Conclusions

The deployment of miniaturized sensors (SF Mini) through a conventional physical model of a Kaplan turbine is feasible to evaluate the magnitudes of hydraulic stressors that affect fish passing through analogous prototypes in operation. This feasibility is attested through three features that were revealed through the present investigation. First, the SF Mini deployments can be conducted with relatively few adaptations of the test rig, namely, the installation of an ingress pipe to introduce sensors, the placement of a mesh to collect sensors at the draft tube end, and the operation at greater Thoma numbers to avoid very low pressures that may damage sensors. Second, the down-time for disassembling and assembling the interrogated physical model for sensor release/retrieval is within an

Table 1
Percentage of significant acceleration events identified as collsions (HBET, peak acceleration greater than 95 g and peak duration less than 7.5 ms).

Region	Time Marks	OP1	OP2	Two-proportion Statistical Test outcome, $\alpha = 0.05$
Intake	T0 to T1	4.3 %	33.3 %	Collision rates are not equal (H_0 was rejected)
Guide vane	T1 to T2	47.8 %	80.0 %	Collision rates are not equal (H_0 was rejected)
Runner	T2 to T3	26.1 %	13.3 %	Collision rates are equal (H_0 was not rejected)
Draft tube	T3 to T4	21.7 %	13.3 %	Collision rates are equal (H_0 was not rejected)

acceptable limit for test rig operations. As such, this feasibility test showed that turbine industry can perform fish passage assessments as a task additional to standard hydraulic testing, instead of having to install an entirely new setup exclusively for fish-related evaluations. Third, the sample sizes collected herein, given time and resource constraints, allow for a statistical analysis of the passage conditions. More importantly, SF data can validate computer-based evaluations and provide a baseline on which improvements in candidate geometries can be pursued. It is nevertheless necessary to generate more passage datasets to test the sensitivity of fish-related outcomes to sample size. This study demonstrated that experiments with SF Mini in commercial test rigs are plausible during the design phase of turbine geometries.

Test rig evaluations of this kind can accelerate the development of the next generation of turbines in which fish-related features take high priority. Industry should see itself as an important player in this process because it is within the design teams and test rigs of turbine manufacturing industries where geometries are iteratively conceived and put to test following strict standards and protocols. This iterative process offers the biggest opportunity for effective changes in the search of fish passage survival improvements.

CRediT authorship contribution statement

Pedro Romero-Gomez: Writing – review & editing, Writing – original draft, Visualization, Resources, Methodology, Investigation, Formal analysis, Data curation, Conceptualization. **Aljon Salalila:** Methodology, Conceptualization. **Z. Daniel Deng:** Writing – review & editing, Software, Methodology, Investigation, Formal analysis, Conceptualization. **Rudolf Peyreder:** Project administration, Methodology, Investigation, Funding acquisition, Conceptualization.

Declaration of competing interest

The authors declare that they have no known competing financial interests or personal relationships that could have appeared to influence the work reported in this paper.

Appendix A. Supplementary data

Supplementary data to this article can be found online at https://doi.org/10.1016/j.heliyon.2024.e26846.

References

[1] S. Amaral, G. Hecker, N. Pioppi, Fish passage through turbines: application of conventional hydropower data to hydrokinetic technologies, Electric Power Res Inst Rep 1024638 (2011) 1–56.
[2] M.S. Bevelhimer, B.M. Pracheil, A.M. Fortner, R. Saylor, K.L. Deck, Mortality and injury assessment for three species of fish exposed to simulated turbine blade strike, Can. J. Fish. Aquat. Sci. 76 (12) (2019) 2350–2363.
[3] C.A. Boys, B.D. Pflugrath, M. Mueller, J. Pander, Z.D. Deng, J. Geist, Physical and hydraulic forces experienced by fish passing through three different low-head hydropower turbines, Mar. Freshw. Res. 69 (12) (2018) 1934–1944.
[4] R.S. Brown, et al., Quantifying mortal injury of juvenile Chinook salmon exposed to simulated hydro-turbine passage, Trans. Am. Fish. Soc. 141 (1) (2012) 147–157.
[5] R.S. Brown, et al., Understanding barotrauma in fish passing hydro structures: a global strategy for sustainable development of water resources, Fisheries 39 (3) (2014) 108–122.
[6] G.F. Čada, The development of advanced hydroelectric turbines to improve fish passage survival, Fisheries 26 (9) (2001) 14–23.
[7] C.C. Coutant, R.R. Whitney, Fish behavior in relation to passage through hydropower turbines: a review, Trans. Am. Fish. Soc. 129 (2) (2000) 351–380.
[8] Z.D. Deng, J. Lu, M.J. Myjak, J.J. Martinez, C. Tian, S.J. Morris, T.J. Carlson, D. Zhou, H. Hou, Design and implementation of a new autonomous sensor fish to support advanced hydropower development, Rev. Sci. Instrum. 85 (11) (2014) 115001.
[9] J. Geist, Green or red: challenges for fish and freshwater biodiversity conservation related to hydropower, Aquat. Conserv. Mar. Freshw. Ecosyst. 31 (7) (2021) 1551–1558.
[10] S.F. Harding, R.P. Mueller, M.C. Richmond, P. Romero-Gomez, A.H. Colotelo, Fish response to turbulence generated using multiple randomly actuated synthetic jet arrays, MDPI Water 11 (8) (2019) 1715.
[11] P.M. Harrison, et al., Turbine entrainment and passage of potadromous fish through hydropower dams: developing conceptual frameworks and metrics for moving beyond turbine passage mortality, Fish Fish. 20 (3) (2019) 403–418.
[12] T.W. Hogan, G.F. Cada, S.V. Amaral, The status of environmentally enhanced hydropower turbines, Fisheries 39 (4) (2014) 164–172.
[13] H. Hou, et al., A hydropower biological evaluation toolset (HBET) for characterizing hydraulic conditions and impacts of hydro-structures on fish, Energies 11 (4) (2018) 990.
[14] I.E.C. Standard, Hydraulic Turbines, Storage Pumps and Pump-Turbines—Model Acceptance Tests, 1999.
[15] E.M. Klopries, H. Schüttrumpf, Mortality assessment for adult European eels (*Anguilla anguilla*) during turbine passage using CFD modelling, Renew. Energy 147 (2020) 1481–1490.
[16] X. Li, Z.D. Deng, R.S. Brown, T. Fu, J.J. Martinez, G.A. McMichael, J.R. Skalski, R.L. Townsend, B.A. Trumbo, M.L. Ahmann, J.F. Renholds, Migration depth and residence time of juvenile salmonids in the forebays of hydropower dams prior to passage through turbines or juvenile bypass systems: implications for turbine-passage survival, Conservation Physiology 3 (1) (2015) cou064.
[17] J.J. Martinez, et al., Characterization of a siphon turbine to accelerate low-head hydropower deployment, J. Clean. Prod. 210 (2019) 35–42.
[18] J.J. Martinez, et al., Hydraulic and biological characterization of a large Kaplan turbine, Renew. Energy 131 (2019) 240–249.
[19] J.J. Martinez, et al., In situ characterization of turbine hydraulic environment to support development of fish-friendly hydropower guidelines in the lower Mekong River region, Ecol. Eng. 133 (2019) 88–97.
[20] J.J. Martinez, Z.D. Deng, R. Mueller, S. Titzler, In situ characterization of the biological performance of a Francis turbine retrofitted with a modular guide vane, Appl. Energy 276 (2020) 115492.
[21] E.F. Moran, M.C. Lopez, N. Moore, N. Müller, D.W. Hyndman, Sustainable hydropower in the 21st century, Proc. Natl. Acad. Sci. USA 115 (47) (2018) 11891–11898.

[22] M.J. Mueller, J. Pander, J. Geist, Evaluation of external fish injury caused by hydropower plants based on a novel field-based protocol, Fish. Manag. Ecol. 24 (3) (2017) 240–255.
[23] M. Mueller, et al., Assessing turbine passage effects on internal fish injury and delayed mortality using X-ray imaging, PeerJ 8 (2020) e9977.
[24] S. Müller, O. Cleynen, S. Hoerner, N. Lichtenberg, D. Thévenin, Numerical analysis of the compromise between power output and fish-friendliness in a vortex power plant, J. Ecohydraulics. 3 (2) (2018) 86–98.
[25] B.M. Pracheil, C.R. DeRolph, M.P. Schramm, M.S. Bevelhimer, A fish-eye view of riverine hydropower systems: the current understanding of the biological response to turbine passage, Rev. Fish Biol. Fish. 26 (2) (2016) 153–167.
[26] M.C. Richmond, J.A. Serkowski, L.L. Ebner, M. Sick, R.S. Brown, T.J. Carlson, Quantifying barotrauma risk to juvenile fish during hydro-turbine passage, Fish. Res. 154 (2014) 152–164.
[27] P. Romero-Gomez, M. Lang, S. Weissenberger, The bio-hill chart of a Kaplan turbine, J. Ecohydraulics. 7 (2) (2022) 94–110.
[28] A. Salalila, Z.D. Deng, J.J. Martinez, J. Lu, L.J. Baumgartner, Evaluation of a fish-friendly self-cleaning horizontal irrigation screen using autonomous sensors, Mar. Freshw. Res. 70 (9) (2019) 1274–1283.
[29] R. Saylor, A. Fortner, M. Bevelhimer, Quantifying mortality and injury susceptibility for two morphologically disparate fishes exposed to simulated turbine blade strike, Hydrobiologia 842 (1) (2019) 55–75.
[30] W.M. Twardek, et al., Bright spots for inland fish and fisheries to guide future hydropower development, Water Biol. Secur. 1 (1) (2022) 100009.
[31] Y. Ventikos, F. Sotiropoulos Jr., R.K. Fisher, P. March, P. Hopping, A CFD framework for environmentally-friendly hydroturbines, Waterpower'99: Hydro's Future: Technology, Markets, and Policy (1999) 1–10.